Mon. Not. R. Astron. Soc. (1992) **259**, 593–603

UV spectroscopy of Z Chamaeleontis – II. The 1988 January normal outburst★

E. T. Harlaftis,[1,2] T. Naylor,[3]†‡ B. J. M. Hassall,[4] P. A. Charles,[1,2] G. Sonneborn[5]§ and J. Bailey[6]

[1]*Royal Greenwich Observatory, Apartado 321, 38780 Santa Cruz de La Palma, Tenerife, Canary Islands*
[2]*Department of Astrophysics, Nuclear Physics Laboratory, Keble Road, Oxford OX1 3RH*
[3]*Institute of Astronomy, Madingley Road, Cambridge CB3 0HA*
[4]*Royal Greenwich Observatory, Madingley Road, Cambridge CB3 0EZ*
[5]*Laboratory for Astronomy and Solar Physics, NASA Goddard Space Flight Center, Code 681, Greenbelt, MD 20771, USA*
[6]*Anglo-Australian Observatory, PO Box 296, Epping, New South Wales 2121, Australia*

Accepted 1992 May 27. Received 1992 April 14; in original form 1992 February 3

ABSTRACT

We present *IUE* observations of the 1988 January normal outburst of Z Cha and compare it with the 1987 April superoutburst (Paper I). The C IV λ1549, Si IV λ1397 and N V λ1240 lines are ~40 per cent weaker than in superoutburst and are all partially eclipsed, by 10–30 per cent, which is similar to the situation during superoutburst. The spectra are bluer than in superoutburst, indicating a less extensive vertical-disc structure during normal outburst. The most dramatic difference from superoutburst is that the outburst continuum flux shows <10 per cent orbital variation away from eclipse, implying that there is no 'cool' bulge on the disc to occult the brighter inner disc periodically. During outburst, the total observed luminosity of Z Cha is two orders of magnitude less than in VW Hyi. We discuss the implications for the outburst mechanism in the two types of outburst. Simultaneous IR observations during the normal outburst reveal the secondary star. Assuming that the secondary is not heated, the disc has brightened by a factor of seven from its quiescent level, and now contributes 75 per cent of the total IR flux, compared to ≲30 per cent during quiescence.

Key words: binaries: close – stars: individual: Z Cha – novae, cataclysmic variables – ultraviolet: stars.

1 INTRODUCTION

This is our second paper on Z Cha, a high-inclination SU UMa system, in which we propose to draw a detailed comparison between normal outbursts and superoutbursts (Harlaftis et al. 1992; hereafter Paper I). This campaign was initiated after limited *IUE* observations of the eclipsing dwarf nova Z Cha suggested substantial spectroscopic differences between the two states of outburst. These individual observations during the decline of the 1985 July superoutburst and during the 1982 January normal outburst (as well as two images from a 1979 normal outburst) were inadequate to form any conclusions. *IUE* observations of OY Car and Z Cha during superoutburst were undertaken, which showed that the UV flux distribution is relatively cool and is modulated on the orbital time-scale, away from eclipse, by the gas-stream impact region, while the UV emission lines are strong and variable (Naylor et al. 1988; Paper I). Z Cha and OY Car had not been systematically observed before with *IUE* during their 2 to 3 day long normal outbursts.

UV spectroscopy during normal outburst and superoutburst is a powerful probe of the triggering mechanism that causes the two types of outburst. The short-lived normal outbursts can be accounted for by an instability, the contro-

★Based on observations by the *International Ultraviolet Explorer* collected at the Villafranca Tracking Station of the European Space Agency and at the Goddard Space Flight Center of the National Aeronautics and Space Administration.
†Previous address: *IUE* Observatory, European Space Agency, Apartado 50727, 28080 Madrid, Spain.
‡Present address: Department of Physics, Keele University, Staffordshire ST5 5BG.
§Previous address: *IUE* Observatory, NASA Goddard Space Flight Center, Greenbelt, MD 20771.

versy being whether this is a disc or a secondary star instability. (For a comparison between the two models, see Verbunt 1986; for a review of the disc instability model, see Smak 1984, Meyer 1985 or Osaki 1989a.) The longer superoutbursts may be the result of prolonged mass transfer from the red dwarf star (Osaki 1985; Bath, Clarke & Mantle 1986; Whitehurst & King 1991). A disc instability combined with either a tidal instability (Osaki 1989b) or a mass transfer burst (Duschl & Livio 1989) has also been claimed to produce a superoutburst. Observationally, the evidence is growing that superoutbursts are triggered from within certain normal outbursts (Bateson 1977; Marino & Walker 1979; Pringle et al. 1987). Here we present *IUE* observations taken during the 1988 January normal outburst of Z Cha and perform a detailed comparison with the 1987 April superoutburst (Paper I). We investigate the evolution of the continuum flux distribution and emission-line fluxes, the modulation of the continuum and line fluxes with orbital phase, and the behaviour of the mid-eclipse spectra during normal outburst. Finally, we discuss results from simultaneous infrared (IR) observations during the 1988 January normal outburst.

2 OBSERVATIONS AND DATA REDUCTION

2.1 *IUE* observations

We obtained good orbital and secular coverage with *IUE* of the 1988 January normal outburst of Z Cha using our Target of Opportunity (TOO) program with *IUE* (see Table 1). The FES estimates have been converted to m_{fes} (Barylak 1989) and are included in Table 1. Figs 1(a) and (b) show the light curve of the *IUE* observations, while Fig. 1(c) shows the visual light curve obtained by the Variable Star Section of the Royal Astronomical Society of New Zealand (VSS RAS NZ) and the FES. The normal outburst rose in 0.6 d, reached a maximum of $V=12.9$ on January 28 and declined in 2 d. The first *IUE* observations started 4.5 h after the optical maximum was reported and caught the UV still rising. They covered roughly 4 h of the late rise at a mean FES magnitude of 12.9 (January 28). The other two groups of observations were carried out 12 and 24 h later and covered about 7 and 5 h at a mean FES magnitude of 13.5 and 14.1 respectively. One 'double' exposure on January 31 was taken to observe Z Cha at the end of the normal outburst (blind offset). We

Table 1. Journal of *IUE* observations of Z Cha during normal outburst.

Date 1988	Start UT h m s	Image No.	mid-HJED (244 0000+)	Exp. (m)	Orbital Phase	FES mag	
Jan 28	16 24 24	LWP12579	7189.18898	15	0.20-0.34	12.95	rise
28	16 44 08	SWP32799	.20442	20	0.39-0.57	13.01	"
28	17 18 18	LWP12580	.22815	20	0.71-0.89	12.84	"
28	17 46 56	SWP32800	.24283	5	0.97-0.02	13.08	peak
28	18 27 15	SWP32801	.27777	25	0.35-0.58	12.78	"
Jan 29	07 07 01	SWP32805	7189.80366	20	0.43-0.67	13.29	early
29	07 36 31	LWP12583	.82415	20	0.71-0.89	13.34	decline
29	08 12 48	SWP32806	.84934	20	0.04-0.23	15.18	"
29	08 48 05	LWP12584	.87385	20	0.37-0.56	13.36	"
29	09 19 55	SWP32807	.89595	20	0.67-0.86	13.41	"
29	09 52 54	LWP12585	.91365	5	0.98-0.02	13.58	"
29	10 21 32	SWP32808	.93874	20	0.24-0.43	13.34	"
29	10 54 14	LWP12586	.96145	20	0.55-0.74	13.43	"
29	11 39 33	SWP32809	.98771	5	0.97-0.02	13.39	"
29	12 22 25	LWP12587	7190.02269	20	0.37-0.56	13.41	"
29	13 02 45	SWP32810	.05070	20	0.75-0.93	13.41	"
29	13 35 05	LWP12588	.07316	20	0.05-0.23	14.61	"
29	14 28 14	SWP32811	.11007	20	0.54-0.73	13.49	"
Jan 30	02 18 43	SWP32814	7190.60521	25	0.17-0.39	14.05	decline
30	02 51 32	LWP12589	.62800	25	0.47-0.70	13.95	"
30	03 24 00	SWP32815	.64881	20	0.77-0.96	13.95	"
30	04 00 34	LWP12590	.67489	22	0.12-0.32	14.08	"
30	04 31 49	SWP32816	.69764	25	0.41-0.64	14.15	"
30	05 32 15	SWP32817	.73266	5	0.97-0.02	14.12	"
30	05 44 12	LWP12591	.74686	22	0.08-0.29	14.23	"
30	06 15 43	SWP32818	.77326	35	0.38-0.70	14.23	"
Jan 31	04 17 18	SWP32827a†	7191.68298	25	0.75-0.98	>14.5	late
31	05 11 02	SWP32827b	.72030	25	0.25-0.48	>14.5	decline
31	06 04 35	SWP32827c	.75749	25	0.75-0.98	>14.5	"
31	06 58 16	SWP32827d	.79477	25	0.25-0.48	>14.5	"
31	07 51 58	SWP32827e	.83207	25	0.75-0.98	>14.5	"
31	08 45 21	SWP32827f	.86914	25	0.25-0.48	>14.5	"
31	09 39 10	SWP32827g	.90652	25	0.75-0.98	>14.5	"

†Note that this is a 'double' exposure obtained at the end of the outburst; the exposures with phase range 0.25–0.48 were obtained with the star on one side of the aperture and the ones with phase range 0.75–0.98 at the other side.

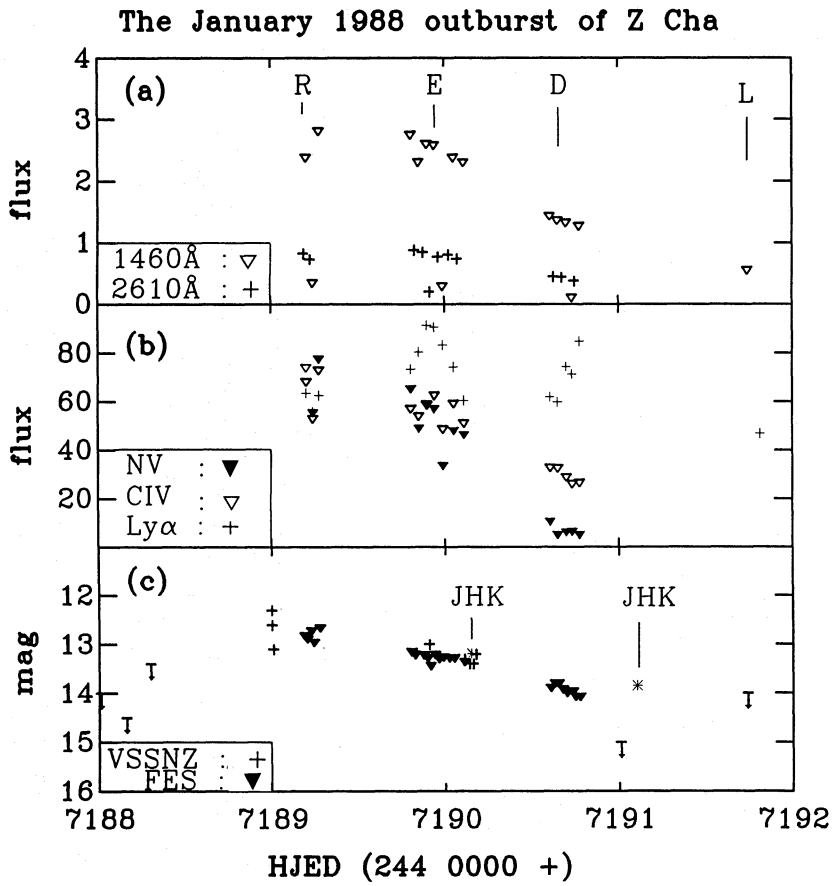

Figure 1. The light curve of Z Cha during the 1988 January normal outburst. (a) is the 1420–1500 Å band (triangles) and the 2580–2640 Å band (crosses) in units of 10^{-13} erg cm^{-2} s^{-1} Å^{-1}. The eclipses can clearly be identified. 'R' shows the late rise, 'E' the early decline, 'D' the decline and 'L' the late decline of the outburst. (b) shows the evolution of N v (filled triangles), C iv (triangles) and Lyman α (crosses) emission lines during the outburst. (c) is the optical estimates as given by the VSS RAS NZ (upper limits and crosses) and the FES camera (triangles). The times of the IR observations are marked. The asterisk shows the *J* magnitude.

obtained in total 13 LWP and 16 SWP spectra using the large aperture in low-resolution mode. For details of the data reduction see Paper I. The SWP spectra were corrected for an absolute-wavelength calibration error reported by Thomson (1989), which caused a −2.5-Å shift for the data discussed here. Fig. 2 shows representative SWP spectra during various stages of the normal outburst. The strong emission lines present during the peak disappear or become weaker as the continuum weakens. Note the transformation of Si iv from emission during the peak to absorption at the end of the normal outburst. We deduce that the geocoronal Lyman α emission accounts for 25 ± 5 per cent of the point source emission, as extracted from line-by-line *IUE* images. The LWP spectra are featureless and their flux evolution is shown in Fig. 1(a).

2.2 Infrared observations

Infrared photometry of Z Cha was obtained using the Infrared Photometer Spectrometer (Barton & Allen 1980) on the 3.9-m Anglo-Australian Telescope. On 1988 January 29, a light curve covering just over one complete cycle was observed in the *H* (1.65 μm) band (Fig. 3), followed by single measurements in the *J* (1.20 μm) and *K* (2.2 μm) bands. On January 30, single measurements were made in each of the *J*, *H* and *K* bands. The photometry is on the AAO system using the standard stars of Allen & Cragg (1983). The times of the AAT observations are marked in Fig. 1 and the IR magnitudes are given in Table 2. Note that the IR flux decays more slowly than the optical flux during the normal outburst.

3 THE INFRARED VARIATION

3.1 The IR light curve

3.1.1 The primary eclipse

Our *H*-band light curve of Z Cha during normal outburst shows a primary eclipse of 0.9 mag (Fig. 3) compared to 1.5 mag in the *V* and *R* bands during normal outburst (Cook 1985), and 0.5 mag in the *J* and *K* bands during quiescence (Bailey et al. 1981). The eclipse half-width $\Delta\phi_{1/2}=0.11$ gives the radius of the disc directly for the known geometry of Z Cha (Sulkanen, Brasure & Patterson 1981), and is found to be similar to the tidal radius, $\sim 0.62\ R_{L_1}$, of Z Cha (see fig. 4 in Whitehurst 1988). This exceeds the disc radius in the optical of $0.5\ R_{L_1}$ during normal outburst (for $\Delta\phi_{1/2}=0.09$; Horne & Cook 1985). The primary IR eclipse shows a slightly slower ingress than

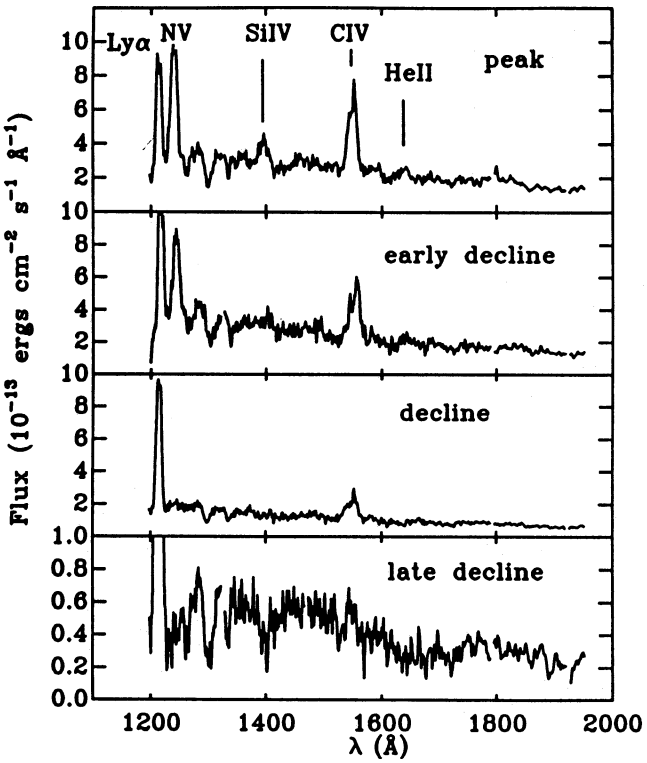

Figure 2. SWP spectra during the 1988 January normal outburst of Z Cha. From top to bottom: peak (SWP32801), early decline (SWP32805), decline (SWP32818) and late decline (SWP32827).

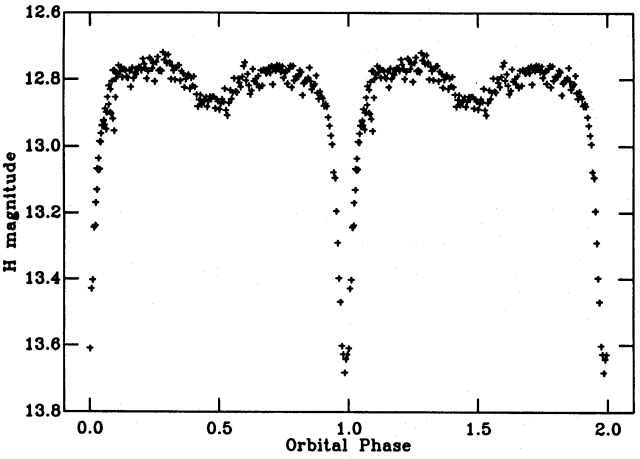

Figure 3. The *H*-band light curve of Z Cha on January 29 folded on the orbital period. Note the deep and wide primary eclipse but also the secondary minimum at phase 0.5 caused by the secondary star. The data are repeated for clarity.

egress, an effect which is more pronounced in OY Car during superoutburst (Naylor et al. 1987). There, it was suggested that the bright spot may be obscuring the disc, causing this early and slow ingress to eclipse.

3.1.2 The secondary eclipse

During quiescence, Bailey et al. (1981) showed that the secondary minimum at orbital phase 0.5 of the IR light curve is caused by the ellipsoidal variations and eclipse of the secondary star by the accretion disc. The secondary star is apparently bright enough even in outburst to produce a secondary minimum of 0.09-mag depth in the *H*-band light curve. Indeed, the decreased importance of the secondary minimum compared with its width and ~0.3-mag depth during quiescence (*J*-band; Bailey et al. 1981) is consistent with the $\Delta J = 1.2$ mag increase of the flux between the two states (see Table 3). The above assumes that the heating of the secondary star in the IR is insignificant during normal outburst.

Alternatively, assuming that no ellipsoidal variations exist, the shape of the light curve can be reproduced by taking into account the effect of a heated, inner face of the secondary in relation to the geometry of the system. A heating effect alone would manifest itself as sinusoidal modulation with a peak at phase 0.5, but as the inner face is partially eclipsed by the accretion disc for this high inclination system, a secondary minimum arises in the IR continuum light curve with the maxima now at phases 0.25 and 0.75. This being true, the secondary minimum should be deeper than observed, adding the above effects together (i.e. ellipsoidal variations and a heated secondary). Thus, we conclude that the ellipsoidal variations are the dominant effects influencing the shape of the light curve. Further, the disc far-UV and soft X-ray emission during outburst is expected to be absorbed before reaching the photosphere of the secondary, creating a relatively hot corona around the inner face of the secondary star rather than heating it (Hameury, King & Lasota 1986). Thereafter, we continue our discussion by considering any heating effects on the secondary as insignificant. During superoutburst, we calculate that the secondary minimum should still be observable in Z Cha and should have a depth of ~0.06 mag in *H*, assuming the system brightens up to 0.5 mag in this band at superoutburst relative to normal outburst (the superoutburst is brighter in the optical by 0.5 mag more than in outburst; Ritter 1990).

No secondary minimum was observed in the IR light curve of OY Car during superoutburst (Naylor et al. 1987), which must be due either to a fainter red star or to a brighter disc than in Z Cha. Using the IR colours $J-H$ and $H-K$ of the secondaries of OY Car and Z Cha in quiescence (Berriman 1984 and Bailey et al. 1981 respectively), we find that the secondary in OY Car is apparently 0.4–0.8 times fainter than in Z Cha. We estimate in the following section that the contribution of the secondary star in Z Cha is ~25 per cent of the IR flux in normal outburst.

3.2 IR contribution from the disc

The above discussion indicates that the disc is the cause of the IR brightness increase during normal outburst. During quiescence, the secondary star contributes ~70 per cent of the *H*-band flux (see fig. 3 in Bailey et al. 1981). Since the IR contribution from the secondary has not significantly changed during normal outburst, and the brightness of the system has increased by a factor of 2.8 during normal outburst from its quiescent flux in *H* ($\Delta H = 1.1$ mag), then the non-secondary IR flux (i.e. disc, bright spot, white dwarf) during normal outburst is $2.8 - 0.7 = 2.1$ times the total quiescent flux in *H*. This means that the disc, which is the main non-secondary IR source, has brightened by a factor of ~7

during normal outburst and increased its IR contribution from $\lesssim 30$ per cent during quiescence to ~ 75 per cent during normal outburst. During normal outburst, the H flux at mid-eclipse is 1.3 times the quiescent flux out-of-eclipse, which indicates that the flux from the uneclipsed part of the disc is 0.4 times the H flux of the secondary star (or 10–15 per cent of the total H flux).

The origin of the IR light in CVs can be investigated in a colour–colour $(H-K,\ J-K)$ diagram (flux-ratio diagram; fig. 2(a) in Berriman, Szkody & Capps 1985). We can deduce the colours of the IR normal-outburst disc from our observations and the known colours of the secondary star (Table 3). Thus we find that, during normal outburst, the ratios $F_\nu(J)/F_\nu(K)=1.91\pm0.08$ and $F_\nu(H)/F_\nu(K)=1.66\pm0.08$ for the disc colours away from eclipse correspond to those of opaque gas at a temperature 6000–8000 K in the flux-ratio diagram. In steady-state discs, such temperatures arise for mass-transfer rates of $\sim 1\times10^{-9}$ $M_\odot$ yr^{-1} (see fig. 2(b) in Berriman et al. 1985). During eclipse, the above ratios become 2.09 and 1.31, which correspond to colours from gas intermediate between optically thin and thick states. This indicates that the outer disc (uneclipsed part) during normal outburst has considerable optically thin emission. The contribution of the optically thin component to the colours away from eclipse is not detected because it is comparable to the uncertainty in the flux ratio method (~ 20 per cent). These findings for the IR continuum in and away from eclipse are consistent with an origin of the IR continuum partly from an opaque gas and partly from optically thin gas as found by Berriman et al. (1985).

Table 2. IR Photometry of Z Cha during normal outburst.

d	h m	mag	HJED	Phase
29 Jan	15 30	J=13.19	7190.150189	0.181
29 Jan	13 50	H=12.76	7190.076340	0.193*
29 Jan	15 33	K=12.68	7190.152273	0.209
30 Jan	14 20	J=13.85	7191.101653	0.953
30 Jan	14 22	H=13.56	7191.103042	0.971
30 Jan	14 25	K=13.27	7191.105126	0.999

*Observations covering one orbital cycle (Fig. 3).

4 THE UV BEHAVIOUR

4.1 The UV continuum

Fig. 1 shows (a) the UV continuum (1420–1500 Å and 2580–2640 Å) and (b) the emission-line light curves. The continuum flux, disregarding those points taken in eclipse, declines smoothly in all three bands, in contrast to the super-outburst, which shows short-term variations which are comparable in size to the secular changes (Paper I). The UV flux in the 1420–1500 Å band still rises (17 ± 2 per cent on a time-scale of one orbital period), while the flux in the 2580–2640 Å band remains at the same level during the late rise-peak of the normal outburst. The UV flux during the early decline of the normal outburst decreases faster than during the late decline. Any UV variability on the orbital period must be less than the secular decline of the normal outburst. For instance, the secular change during the early decline of the normal outburst causes a 10 per cent variation of the mean out-of-eclipse flux on the orbital time-scale. Thus, with the exception of eclipse effects, no significant phase variation is found for the UV continuum during normal outburst. The eclipse depth of the continuum is 90 per cent for the 1420–1500 Å band and 75 per cent for the 2580–2640 Å band during early decline, indicating an increasingly hotter disc towards the compact object, as expected.

4.2 The UV emission lines

4.2.1 Time evolution of the emission lines

Fig. 1(b) shows the time evolution of the most prominent emission lines, namely C IV λ1549, N V λ1540 and Lyman α. The strength of these lines is decreasing faster than the UV continuum (see Table 4). Further, the N V emission decays faster than C IV, indicating that the ionization decreases. Eclipse of the resonance lines is most significant at the peak of the normal outburst and is ~ 30 and ~ 20 per cent for N V and C IV respectively. The Si IV line is strong only during the rise. He II is occasionally measurable during the rise and the early decline, but generally is very weak. The secular evolution of Lyman α is very different from that of the resonance lines and the continuum. We estimate that the geocoronal contribution can account for up to 20–30 per cent of the Lyman α flux and it is thus quite possible to affect its secular evolution. Spectra in the decline show traces of

Table 3. IR colours of Z Cha during outburst and quiescence.

	J	H	K	J–H	H–K	$F_\nu(J)/F_\nu(K)$	$F_\nu(H)/F_\nu(K)$
quiescence*	14.36	13.89	13.54	0.47	0.36	1.19	1.15
secondary*	14.70	14.16	13.80	0.54	0.36	1.07	1.12
outburst	13.19	12.76	12.68	0.43	0.08	1.58	1.47
" (e)	13.85	13.56	13.27	0.29	0.29	1.49	1.21
outburst disc	13.47	13.11	13.16	0.36	-0.05	1.91	1.66
" (e)	14.51	14.49	14.30	0.02	0.19	2.09	1.31

*Adopted from Bailey et al. (1981).
$F_\nu(i)$ is the flux density at band i and (e) are observations during eclipse on January 30. The other magnitudes were measured at phase ~ 0.3.

Table 4. Equivalent widths and UV line fluxes of Z Cha during outburst.

SWP	CIV λ 1549		NV λ 1240		Lyman α	
No.	EW Å	flux	EW Å	flux	EW Å	flux
32799	33±1	6.8±0.2	39±1	7.4±0.2	38±1	6.3±0.2
32800	29±1	5.3±0.6	69±14	5.6±0.4	65±17	5.6±0.6
32801	158±44	7.3±0.2	26±1	7.8±0.2	21±1	6.3±0.2
32805	24±1	5.7±0.2	20±1	6.6±0.3	22±1	7.3±0.4
32806	27±1	5.4±0.2	18±1	4.9±0.2	28±1	8.0±0.3
32807	25±1	5.9±0.2	20±1	5.9±0.2	29±1	9.1±0.3
32808	28±1	6.3±0.2	19±1	5.7±0.2	23±1	9.1±0.3
32809	162±14	4.9±0.6	130±36	3.4±0.4	351±58	8.3±0.6
32810	28±1	5.9±0.2	17±1	4.8±0.2	25±1	7.4±0.3
32811	26±1	5.1±0.2	19±1	4.7±0.2	20±1	6.0±0.2
32814	26±1	3.3±0.2	6±1	1.1±0.1	31±1	6.2±0.2
32815	27±1	3.3±0.2	3±1	0.52±0.1	34±1	6.0±0.2
32816	24±1	2.9±0.2	-	-	43±1	7.4±0.2
32817	223±32	2.6±0.4	-	-	388±80	7.1±1.5
32818	24±1	2.7±0.6	-	-	49±1	8.5±0.2

The flux is in units of 10^{-12} erg cm^{-2} s^{-1}.

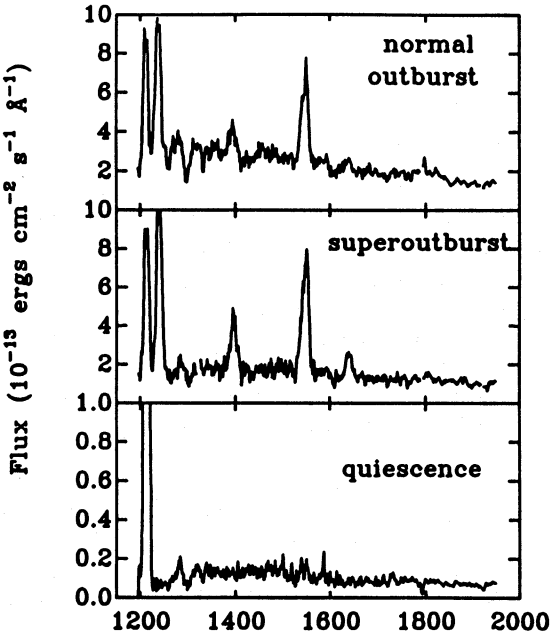

Figure 4. Representative spectra from quiescence (SWP28262), normal outburst (SWP32801; peak) and superoutburst (SWP30706; plateau). The FES magnitude is 12.65 and the orbital phase is ~0.5 for both outburst spectra.

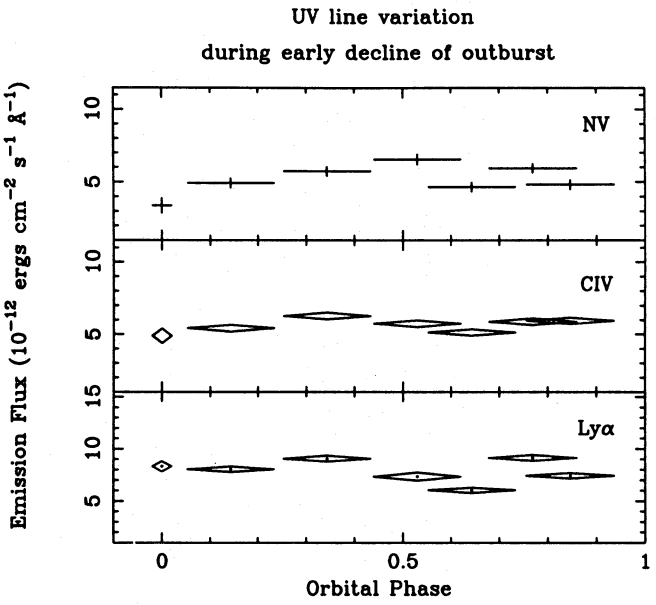

Figure 5. The UV line fluxes on 1988 January 29 are plotted as a function of orbital phase. The vertical extent of each point is the uncertainty for that point, while the horizontal extent is the exposure duration.

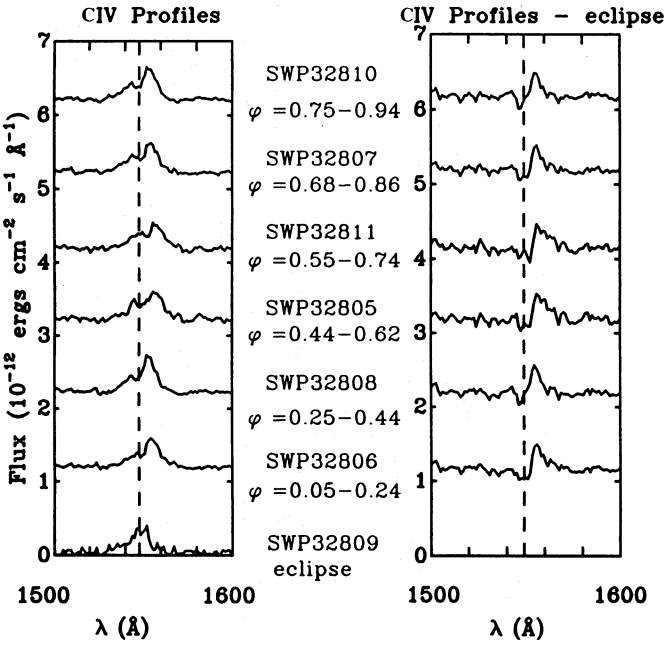

Figure 6. The left panel shows the C IV profiles on January 29 arranged to ascend in orbital phase. The right panel shows the results of subtracting the profile in eclipse from all the other profiles away from eclipse.

N V and relatively weak C IV emission. Near the end of the normal outburst, while the continuum is still stronger than its quiescent level by a factor of six, Si IV is then in absorption (compare the late-decline spectrum in Fig. 2 with the quiescent spectrum in Fig. 4).

4.2.2 *Variability on the orbital time-scale*

Fig. 5 presents the emission-line behaviour of the most prominent lines on the orbital period during the early decline of the normal outburst. Careful examination of Fig. 1(b) and Fig. 5 shows that, except for the eclipse, the N V and C IV line variation is dominated by the secular evolution. Lyman α shows no orbital modulation, not even an eclipse. Fig. 6 shows the C IV profiles during the early decline of the normal outburst plotted in order of increasing orbital phase. They are very asymmetric and a secondary, blue peak appears, being more distinct at phase 0.5. The difference between

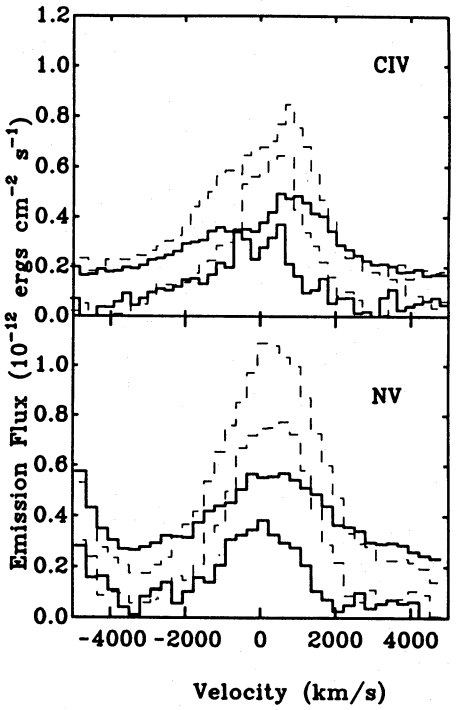

Figure 7. The C IV and N V profiles away from eclipse and in eclipse during normal and superoutburst versus velocity. The solid lines show the profiles during normal outburst (1988 January 29). The dashed lines show the superoutburst profiles (1987 April 5).

these profiles and the eclipse profile is displayed in Fig. 6 (right panel), which shows a weak central absorption feature and a red-emission component. The eclipse profiles of N V and C IV are displayed, relative to their mean out-of-eclipse profiles, in Fig. 7 (solid lines). Most noticeable is the change of the C IV profile during eclipse with loss of the red wing. The superoutburst profiles are also included for comparison (dashed lines).

5 FLUX DISTRIBUTION COMPARED WITH SUPEROUTBURST

The observations we present here and in Paper I show spectroscopic differences between normal outbursts and superoutbursts in high-inclination systems, whereas this is not the case in low-inclination SU UMa systems (Verbunt et al. 1987). This normal outburst of Z Cha revealed strong blue UV spectra with prominent emission lines, whereas observations of low-inclination SU UMa systems have shown similar blue continuum spectra (VW Hyi, Verbunt et al. 1987; SU UMa, Woods, Drew & Verbunt 1990), but with absorption lines. During superoutburst, the high-inclination SU UMa systems have revealed weaker continuum spectra, with stronger emission lines than during normal outburst (OY Car, Naylor et al. 1988; Z Cha, Paper I). Fig. 4 shows representative SWP spectra for Z Cha of the two types of outburst and during quiescence. The cooler flux distribution during superoutburst (see continuum ratios in Table 5) is

Table 5. The UV continuum and line fluxes of Z Cha during normal outburst and superoutburst.

April 1987 superoutburst

	31 Mar			2 Apr			5 Apr			7 Apr		
	m-o-e	eclipse	%	m-o-e	eclipse	%	m-o-e	eclipse	%	m-o-e	eclipse	%
1460 Å	3.53	0.78	78	2.38	0.50	79	2.18	0.20	90	2.53	0.60	76
2610 Å	1.35			0.86			0.72	0.18	75	0.86	0.26	70
Ly α	37	44		88	90	0	91	71	20	70	60	15
N V	128	99	23	106	76	28	118	80	32	63	53	16
Si IV	41	27	34	37	22	40	39	28	28	25	10	60
C IV	95	84	12	90	64	29	99	76	23	73	54	26
He II	7			12	<0.6	<50	16	<8	<50	<4		

January 1988 normal outburst

	28 Jan			29 Jan			30 Jan			error	
	m-o-e	eclipse	%	m-o-e	eclipse	%	m-o-e	eclipse	%	m-o-e	eclipse
1460 Å	2.60	0.36	86	2.49	0.30	88	1.36	0.12	91	0.1	0.3
2610 Å	0.78			0.81	0.20	75	0.42			0.02	0.03
Ly α	63	56	10	78	83		70	71		4	6
N V	76	56	25	54	34	37	<3			3	5
Si IV	22	23	0	7	d					2	5
C IV	69	53	23	56	49	15	30	26	15	3	6
He II	5.5			6.1						2	4

The fluxes are in units of 10^{-13} erg cm^{-2} s^{-1} Å^{-1}. The table gives mean out-of-eclipse flux, flux in eclipse and the eclipse depth for each date. Typical errors in- and out-of-eclipse are given in the two columns on the right, for both outbursts. A blank indicates that no significant detection of the line was made. Note that the line-flux eclipse is deeper in normal outburst than in superoutburst.

Table 6. Flux distribution of Z Cha during the 1988 January normal outburst.

SWP	LWP	$\log f_{1460}$	$\log \frac{f_{1460}}{f_{1800}}$	$\log \frac{f_{1460}}{f_{2300}}$	$\log \frac{f_{1460}}{f_{2880}}$	FES mag
32799	12579	0.377	0.171	0.363	0.495	12.85
32805	12583	0.440	0.214	0.394	0.570	13.17
32807	12584	0.416	0.179	0.371	0.568	13.24
32808	12586	0.412	0.189	0.374	0.596	13.25
32810	12587	0.378	0.178	0.431	0.563	13.27
32814	12589	0.158	0.169	0.380	0.612	13.84
32815	12590	0.137	0.172	0.431	0.577	13.85
32818	12591	0.107	0.189	0.436	0.585	14.06
32827		-0.253	0.239			>14.5

f_i is in units of 10^{-13} erg cm^{-2} s^{-1} Å^{-1}. The typical flux error is 3–4 and 1–2 per cent for the 1460- and 2880-Å lines respectively. See also for explanation table 11 in Paper I.

confirmed by the lower observed UV fluxes for the same FES magnitude. The spectral index of a power-law fit to the continuum decreases during the rise to normal outburst from $\alpha = -1.66 \pm 0.05$ to -1.85 ± 0.05, showing that the spectra become bluer, reaching a spectral index of -2.00 ± 0.05 after the peak. This can be compared with the superoutburst spectral indices of -1.54 ± 0.21 (Z Cha) and -2.25 ± 0.22 (VW Hyi; see Paper I). Table 6 gives the secular evolution of the flux distribution of the normal outburst. The normal-outburst spectra of Z Cha during late rise are as cool as during superoutburst and after the peak become as blue as in VW Hyi during normal outburst. The mean optical flux as measured by the FES has dropped by 30 per cent on the second day of the normal outburst, whereas the UV flux has not followed such a decrease, possibly because of the UV delay on the rise to normal outburst. During superoutburst, the optical and UV fluxes have simultaneously decreased by 30 per cent, 5 d after the peak (Paper I).

Table 7 displays the luminosities during the three states of Z Cha: quiescence, outburst and superoutburst. The relative contribution from each observed band is given in Table 8. During quiescence, the spectral distribution is much flatter than in outburst. During superoutburst, the contribution of the far-ultraviolet to the overall luminosity decreases, whereas the contribution of the optical increases, compared to the outburst. This is consistent with our picture below, where the far-UV (1200–2000 Å) is reprocessed in a more vertically extended disc than in normal outburst and re-emitted in longer wavelengths (2000–7000 Å). The luminosity of the system increases by ~20 times during normal outburst. The observed luminosity during peak of superoutburst is ≈1.3 times that of the normal outburst maximum, indicating an increase of the accretion rate relative to that during normal outburst. We note that, during outburst, the total luminosity of Z Cha is two orders of magnitude less than VW Hyi (or that expected from standard accretion theory), whereas it is similar to that of OY Car (see fig. 9 of Paper I). This suggests that the low luminosity of Z Cha could be mainly an inclination effect (i.e. cos 83° = 0.14).

For VW Hyi, the ratio of the total energy detected during the superoutburst to that detected during the normal outburst E_{SO}/E_O was found to be ≈9, and the time-averaged ratio ≈0.8 (Pringle et al. 1987). In comparison,

Table 7. Energetics of Z Cha.

	quiescence ($\times 10^{30}$ erg s^{-1})	outburst ($\times 10^{31}$ erg s^{-1})	superoutburst ($\times 10^{31}$ erg s^{-1})	band width Å
L_X	1.7	0.078	≤2.1	80
L_{UV_S}	9.2	21.5	24.2	700
L_{UV_L}	4.3	14.4	21.8	1250
L_{FES}	4.8*	9.00	15.0	2500
L_{IR}	5.2	1.39	–	3000
L_{total}	$0.007L_\odot$	$0.12L_\odot$	$0.16L_\odot$	

*White-light flux as observed by Wood et al. (1986).

The luminosities were obtained using a distance of $d = 100$ pc for Z Cha (Wood et al. 1986) for the wavelength bands quoted. The luminosities in quiescence were obtained from an *Einstein* Observation (Becker 1981), *IUE* archive images, and optical (Wood et al. 1986) and IR observations (Bailey et al. 1981). For the outbursts, L_i (i = UV, FES, IR) is the luminosity at peak. L_X was estimated assuming a spectrum with $kT = 10$ keV and $N_H = 1 \times 10^{20}$ cm^{-2} (or $E(B-V) \lesssim 0.05$). The superoutburst X-ray luminosity is at the detection limit of the *EXOSAT* LE telescope; the other fluxes are from the *Einstein* IPC. The UV bands are defined by the wavelength ranges covered by the SWP (1200–1900 Å) and LWP (2100–3150 Å) cameras on *IUE*. The IR luminosity was corrected for an atmospheric extinction of ~0.2 mag (Allen & Cragg 1983).

Table 8. The distribution of luminosity of Z Cha.

	quiescence %	outburst %	superoutburst %
Ratio	1	18	24
X-ray	7	≤1	≤1
UV_S	37	46	40
UV_L	17	31	35
FES	19*	19	25
JHK	21	3	–

*White-light flux as observed by Wood et al. (1986).

we find $E_{SO}/E_O = 4.5$ for Z Cha. The time-averaged ratio is $(E_{SO}/E_O) \times (82/287) \approx 1.3$, where 82 and 287 are the average normal-outburst and superoutburst cycles in days (Ritter 1991).

6 COMPARISON WITH THE UV CONTINUUM DURING SUPEROUTBURST

6.1 The outburst disc is not vertically extended

The relatively cool superoutburst spectra have been interpreted in previous work (Naylor et al. 1988; Paper I) as caused by extended vertical structure of the superoutburst disc. A large opening angle of the disc would partially obscure the central, hot regions in high-inclination systems like Z Cha, thereby giving an observed cooler flux distribution. We therefore suggest that the spectra are bluer during normal outburst because the hot, inner-disc regions are not obscured by the outer disc. This implies that there is a much smaller increase in the opening angle of the disc during

normal outburst compared to superoutburst, and hence that the disc structure during superoutburst has changed significantly compared to the disc during normal outburst.

6.2 The normal outburst disc height does not vary

The UV dips observed during 1987 April superoutburst were associated with azimuthal variation of the height of the disc. In Paper I, we discussed the possibility of mass transfer from the secondary, during at least some of the plateau phase of the superoutburst, being responsible for thickening the disc during superoutburst. The 'hot' spectrum during normal outburst implies a thinner disc than during superoutburst, and the absence of dips implies an insignificant stream-impact region compared to that during superoutburst. The lack of azimuthal variation observed during normal outburst indicates that the vertical structure at phase 0.8 is not extended enough to obscure the inner disc, which implies that the mass transfer rate from the secondary star during normal outburst is less than during superoutburst.

6.3 Other observations

Warner & O'Donoghue (1988; fig. 1) and Kuulkers et al. (1991) have reported the occurrence of optical dips during superoutburst, whereas Cook (1985; fig. 1) observed no optical dips during the 1983 March normal outburst of Z Cha. Indirect evidence for differences in the disc structure between normal outburst and superoutburst may be obtained from maximum-entropy eclipse maps (Horne 1985). The resulting surface-brightness distribution for the superoutburst shows an inversion in the outer parts of the disc (Warner & O'Donoghue 1988), which indicates an extended outer rim (i.e. $H/R^{3/2} \propto T^{1/2}$ from steady-state theory). During normal outburst, the radial brightness temperature distribution shows that the light is more concentrated towards the centre of the disc ($\sim 40\,000$ K), smoothly decreasing towards the outer disc (~ 8000 K at about 0.5 R_{L_1}) (Horne & Cook 1985). Nevertheless, Warner & O'Donoghue (1988) have found a temperature inversion in the outer disc which is also present during (maximum of) normal outburst, although it is less significant than that found during superoutburst. They suggested that this resulted from a very shallow eclipse compared to the eclipse (at early decline of normal outburst) used by Horne & Cook (1985). We note that the temperature inversion shown from the superoutburst eclipse mapping is probably caused by the lack of inner-disc flux, which is hidden by the vertical structure at the edge of the disc, and not by a brighter outer disc as interpreted by Warner & O'Donoghue (1988).

6.4 The outburst model

A promising interpretation of the two distinct states of outburst in SU UMa systems is given by Whitehurst's tidal model (1988). A period of high mass transfer from the secondary may prolong an outburst for the duration of a superoutburst. The growth rate of the superhump during a superoutburst depends critically upon the perturbation effect of increased mass transfer on the outer disc (Whitehurst & King 1991). A normal outburst, which may well be the trigger of the superoutburst, can result from an instability in which the disc changes from a low to a high state. The superoutburst disc has sufficient time to evolve viscously to the tidal radius of the disc after the enhanced mass-transfer event. The tidal influence of the secondary star then distorts the outer disc into an elliptical one, giving rise to the superhump. The tides raised on the outer disc heat it, and possibly increase its vertical extent. The short duration of the normal outburst prevents the disc from growing viscously to its tidal radius and becoming unstable.

7 COMPARISON WITH THE EMISSION LINES DURING SUPEROUTBURST

The UV emission lines that were observed during superoutburst are present, though weaker, in the late rise to normal outburst. After the peak, the resonance lines decline faster than the continuum and have almost disappeared, except for a weak C IV line, during the decline of the normal outburst. While the UV continuum is still quite strong, the wind-driving mechanism must have become significantly less efficient before the end of the normal outburst. The relative strengths of C IV, N V and Si IV between normal outburst and superoutburst are identical only during rise and peak (see Table 5). Of these, the C IV ratio is the highest, its strength during normal outburst being 70 per cent of that during superoutburst, and similar to the continuum flux ratio between the two outbursts (Table 9). This implies that the C IV population during outburst peak is the only one similar to that in superoutburst peak. The total UV line flux from normal outburst to superoutburst shows a similar increase (i.e. 1.3 times) as is seen in the continuum. In addition, the flux ratio of emission line to continuum is ~ 0.1 during both outburst states, indicating that the medium through which the continuum photons are scattered (i.e. the wind) is similar.

The difference between the C IV profiles and those during eclipse reveals different profiles between normal outburst ('single-peaked') and superoutburst ('double-peaked'). The weak central absorption feature can be ascribed to the expected profile behaviour during eclipse (see Paper I). It may well be that, because the system does not have an inclination of exactly 90°, the red-shifted emission compon-

Table 9. Ratios of UV continuum and lines between outburst and superoutburst.

	rise	peak
1460 Å	0.74	0.74
2610 Å	0.58	0.60
Ly α	1.70	0.86
N V	0.59	0.59
Si IV	0.54	0.54
C IV	0.73	0.72
He II	0.80	0.38

Rise ratio is the ratio of normal-outburst fluxes to superoutburst fluxes during rise. Peak ratio is the same ratio but for the highest fluxes observed instead of the rise fluxes.

ent of a ~5000 km s^{-1} wind is eclipsed more than the blue-shifted one. For the 82° inclination of Z Cha, this corresponds to a ~3–4 Å blueward shift for the red part of the profile. The blue part of the profile is also shifted bluewards by ~3–4 Å, because the projected disc-absorbing area is eclipsed (see discussion in section 4.1.1 of Paper I). The above two effects result in a shift of the profile similar to that observed during eclipse.

During the main part of the superoutburst, the C IV and N V emission lines showed shallow eclipses (25 per cent) compared to the deep eclipses of Si IV and He II (Table 5). During eclipses in both outburst states, we found no significant decrease in the FWZI compared to the 30 per cent decrease of the FWHM of the line profiles. The line-forming region must, therefore, have the size of the occulting secondary star with an ionization structure of a He^+ zone in the inner part and of an N^{4+}–C^{3+} zone in the outermost region. During normal outburst, the C IV and N V emission lines also show shallow eclipses (20 and 30 per cent respectively). In OY Car, the eclipses of the C IV and N V lines are deeper than Z Cha (40 and 50 per cent respectively; Naylor et al. 1988).

Hoare & Drew (1991) used the Zanstra method and He II λ1640 to constrain the boundary-layer temperatures in eclipsing dwarf novae and found, from the observations of Z Cha presented here and in Paper I, a slightly higher temperature during superoutburst of ~65 000 K compared to 55 000 K during normal outburst. This suggests that the accretion rate during superoutburst is ~2 times higher than during normal outburst, which is consistent with the observed 0.5-mag difference in optical luminosity between the two outburst states.

8 CONCLUSIONS

The *IUE* TOO programs have enabled us to follow the evolution of the continuum flux distribution and emission-line fluxes during a normal outburst and a superoutburst from the late rise back to quiescence. We have determined the variability of the continuum and emission-line fluxes with orbital phase and analysed the mid-eclipse spectra, and draw the following conclusions.

(i) A bluer flux distribution is observed in normal outburst than in superoutburst, suggesting a thinner disc structure.

(ii) We detect no significant orbital variation, other than eclipse, in the UV normal outburst flux, compared to the complex UV superoutburst flux modulation.

(iii) The orbital variation in the optical is similar to the UV; during normal outburst, the phase variation is limited, whereas during superoutburst, a modulation is observed at phase 0.8.

(iv) During normal outburst, the UV emission lines are 30, 40 and 45 per cent weaker than during superoutburst, for C IV, N V and Si IV respectively.

(v) During normal outburst, a secondary minimum is seen in the *H*-band light curve at phase 0.5, showing that the secondary star is still visible. This is caused by the ellipsoidal variations and eclipse of the red dwarf by the accretion disc. The secondary star has not previously been observed directly in an SU UMa-type dwarf nova during outburst.

We observed the time evolution of the disc during normal outburst and superoutburst and found that the disc structure is different in normal outburst and superoutburst, as implied by the different continuum slopes and continuum flux modulation. The observations showed that enhanced mass transfer from the secondary star is evident from the late rise to superoutburst, whereas no similar evidence was found for the normal outburst. Thus, we conclude that the mass-transfer rate is crucial in distinguishing a superoutburst from a normal outburst.

ACKNOWLEDGMENTS

We thank the *IUE* Observatory staff for scheduling the target of opportunity observations at short notice. Our thanks go to Frank Bateson and the Variable Star Section of the Royal Astronomical Society of New Zealand, whose efforts made this difficult project possible. ETH acknowledges the support of a British Council Scholarship and thanks Tom Marsh and the referee for their useful comments.

REFERENCES

Allen D. A., Cragg T. A., 1983, MNRAS, 203, 777
Bailey J., Sherrington M. R., Giles A. B., Jameson R. F., 1981, MNRAS, 196, 121
Barton J. R., Allen D. A., 1980, PASP, 92, 368
Barylak M., 1989, ESA *IUE* Newsletter, 33, 20
Bateson F. M., 1977, New Zealand J. Sci., 20, 73
Bath G. T., Clarke C., Mantle V. J., 1986, MNRAS, 221, 269
Becker R. H., 1981, ApJ, 251, 626
Berriman G., 1984, MNRAS, 210, 223
Berriman G., Szkody P., Capps R. W., 1985, MNRAS, 217, 327
Cook M. C., 1985, MNRAS, 216, 219
Duschl W. J., Livio M., 1989, A&A, 209, 183
Hameury J. M., King A. R., Lasota J. P., 1986, A&A, 162, 71
Harlaftis E. T., Hassall B. J. M., Naylor T., Charles P. A., Sonneborn G., 1992, MNRAS, 257, 607 (Paper I)
Hoare M. G., Drew J. E., 1991, MNRAS, 245, 452
Horne K., 1985, MNRAS, 213, 129
Horne K., Cook M. C., 1985, MNRAS, 214, 307
Kuulkers E., van Amerongen S., van Paradijs J., Rottgering H., 1991, A&A, 252, 605
Marino B. F., Walker W. S. G., 1979, in Bateson F. M., Smak J., Urch I. H., eds, Proc. IAU Colloq. 46, Changing Trends in Variable Star Research. p. 29
Meyer F., 1985, in Proc. ESA Workshop, Recent Developments on Cataclysmic Variables. ESA SP-236, Bamberg, p. 83
Naylor T., Charles P. A., Hassall B. J. M., Bath G. T., Berriman G., Warner B., Bailey J., Reinsch K., 1987, MNRAS, 229, 183
Naylor T., Bath G. T., Charles P. A., Hassall B. J. M., Sonneborn G., van der Woerd H., van Paradijs J., 1988, MNRAS, 231, 237
Osaki Y., 1985, A&A, 144, 369
Osaki Y., 1989a, in Meyer F. et al., eds, NATO ASI Series C, 290, Theory of Accretion Disks. Kluwer, Dordrecht, p. 183
Osaki Y., 1989b, PASJ, 41, 1005
Pringle J. E. et al., 1987, MNRAS, 225, 73
Ritter H., 1990, A&AS, 85, 1179
Smak J., 1984, PASP, 96, 5
Sulkanen M. E., Brasure L. W., Patterson J., 1981, ApJ, 244, 579
Thomson R., 1989, ESA *IUE* Newsletter, 32, 46
Verbunt F., 1986, in Mason K. O., Watson M. G., White N. E., eds, Physics of Accretion onto Compact Objects. Springer-Verlag, Berlin, p. 59

Verbunt F., Hassall B. J. M., Pringle J. E., Warner B., Marang F., 1987, MNRAS, 225, 113
Warner B., O'Donoghue D., 1988, MNRAS, 233, 705
Whitehurst R., 1988, MNRAS, 232, 35
Whitehurst R., King A., 1991, MNRAS, 249, 25
Wood J., Horne K., Berriman G., Wade R., O'Donoghue D., Warner B., 1986, MNRAS, 219, 629
Woods J. A., Drew J. E., Verbunt F., 1990, MNRAS, 245, 323